

# Testing for flow in the north polar layered deposits of Mars using radar stratigraphy and a simple 3D ice-flow model

N. B. Karlsson,<sup>1</sup> J. W. Holt,<sup>2</sup> and R. C. A. Hindmarsh<sup>3</sup>

Received 11 September 2011; revised 4 November 2011; accepted 8 November 2011; published 22 December 2011.

[1] The water-ice-rich north polar layered deposits (NPLD) of Mars play a key role in the Martian climate through an active exchange of water vapor with the atmosphere. Conditions are not currently amenable for flow of the NPLD; however, gross morphological evidence for past flow suggests the possibility of a warmer climate in the past. Here we present the first comparison of internal stratigraphy predicted by a flow model with that observed by an orbital radar sounder. We have analyzed radar data from Gemina Lingula, the southernmost tongue of the NPLD, acquired by the Shallow Radar on board NASA's Mars Reconnaissance Orbiter. The data shows extensive internal reflections and several radar reflectors were mapped to create gridded surfaces of this part of the NPLD. All the mapped radar reflectors were smooth with no sudden dips towards the surface or the bedrock. The internal radar reflectors were then compared with modeled isochrones in two different areas of Gemina Lingula under the assumption of flow occurring. Results indicate that flow of ice is unlikely to have occurred between the main dome and Gemina Lingula. Furthermore, we found no evidence for the existence of a prior ablation zone in Gemina Lingula as predicted in another study. **Citation:** Karlsson, N. B., J. W. Holt, and R. C. A. Hindmarsh (2011), Testing for flow in the north polar layered deposits of Mars using radar stratigraphy and a simple 3D ice-flow model, *Geophys. Res. Lett.*, 38, L24204, doi:10.1029/2011GL049630.

## 1. Introduction

[2] The north polar layered deposits (NPLD) comprise one of the largest reservoirs of surface water on Mars, but until recently our knowledge of the physical properties of the NPLD has been limited to surface exposures, and the age of the NPLD is still not well constrained [Fishbaugh *et al.*, 2008; Phillips *et al.*, 2008]. Compared with the underlying and surrounding Vastitas Borealis Formation, the surface of the NPLD is geologically young [Tanaka *et al.*, 2008] though some resurfacing processes could be present [Herkenhoff and Plaut, 2000]. It is clear, however, that through an active exchange of water vapor with the atmosphere, the NPLD plays an important role in the Martian climate. Thus, in order to gain insight into past and present Martian climate an increased understanding of the pro-

cesses influencing the NPLD is critical [Clifford *et al.*, 2000; Fishbaugh *et al.*, 2008].

[3] The surface of the NPLD is characterized by an overall domal shape and a spiraling pattern caused by troughs and scarps that expose layers (Figure 1a, inset). Radar sounding has now revealed that the layers exposed in NPLD scarps are continuous over hundreds of kilometers, extending into the interior and throughout the depth of the ice [Phillips *et al.*, 2008]. The stratigraphy and morphology of internal radar reflectors in ice sheets reflect the conditions under which they have been deposited [e.g., Paren and Robin, 1975] and it has been demonstrated that the radar reflectors may be used to obtain information on past accumulation rates and flow history of the NPLD [Koutnik *et al.*, 2009]. In recent years the impact of ice flow on the overall shape of the NPLD has been widely debated (see Byrne [2009] for review). Some studies have concluded that the upper part of the NPLD shows no evidence of flow [Fishbaugh and Hvidberg, 2006] and that surface mass balance alone can produce the topography [Greve *et al.*, 2004; Greve and Mahajan, 2005], while other studies have argued for flow [e.g., Herkenhoff *et al.*, 2007; Fisher *et al.*, 2010]. Perhaps the most compelling evidence for ice flow has been found in Gemina Lingula (GL, also referred to as Titania Lobe [Pathare and Paige, 2005]), the smaller lobe of Planum Boreum (Figure 1a), where relict flow paths were determined [Winebrenner *et al.*, 2008]. We therefore focus our study on GL.

[4] The majority of the radargrams retrieved from the NPLD show packages of numerous radar reflectors interspersed with almost reflection-free zones. This paper is based on analysis of several radar reflectors identified in over 80 radargrams crossing GL (Figure 1a, inset) using the terrestrial approach of mapping the stratigraphy of internal radar reflectors to recover ice sheet history [e.g., Siegert *et al.*, 2003; Rippin *et al.*, 2006; Karlsson *et al.*, 2009]. Based on this dataset we (i) analyze the stratigraphy of the internal radar reflections in GL, (ii) investigate the potential impact of ice flow on the reflectors using a three-dimensional flow model, and (iii) test the hypothesis of an ablation zone in the western part of GL. Because the flow model is three-dimensional, we do not need to make any assumptions about the position of potential flowlines but can follow the acquired radar lines directly.

## 2. Data and Methods

[5] The Shallow Radar (SHARAD) sounder on-board NASA's Mars Reconnaissance Orbiter (MRO) was launched with the aim of mapping subsurface interfaces due to changes in dielectric properties [Seu *et al.*, 2007]. SHARAD operates with a 20-MHz center frequency and a 10-MHz

<sup>1</sup>Centre for Ice and Climate, Niels Bohr Institute, University of Copenhagen, Copenhagen, Denmark.

<sup>2</sup>Institute for Geophysics, Jackson School of Geosciences, University of Texas at Austin, Austin, Texas, USA.

<sup>3</sup>British Antarctic Survey, Cambridge, UK.

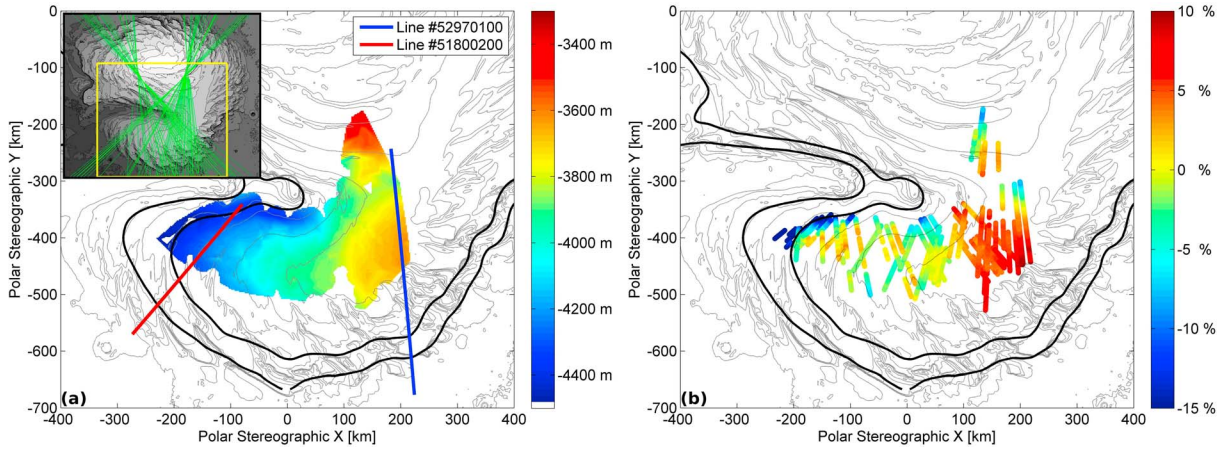


**Figure 1.** (a) Elevation of one of the middle radar reflectors (the reflector is indicated with a magenta arrow in Figure 2). The inset shows NPLD elevation map with all analyzed SHARAD radarlines in green. (b) Difference between the same radar reflector and modeled isochrones for ELA =  $-4200$  m (and internal deformation) in percentage (local) ice thickness. Positive values indicate that the model is underestimating isochrone elevations (as is the case in Figure 2). In both panels the NPLD surface topography is indicated with thin, gray 200 m contour lines (MOLA data [Smith *et al.*, 2001]) while thick, black contour lines show the ELAs for  $-4200$  m and  $-3800$  m that are used in the model.

bandwidth, resulting in a vertical resolution of  $\sim 9$  m in water ice, and after processing, a horizontal resolution of  $\sim 300$  m along-track and 3–6 km cross-track [Seu *et al.*, 2007]. SHARAD has retrieved numerous radargrams from the NPLD used to map its internal structure and large-scale stratigraphy [e.g., Phillips *et al.*, 2008; Putzig *et al.*, 2009; Holt *et al.*, 2010]. Studies based on SHARAD data have shown that to a good approximation the NPLD can be assumed to have a bulk dielectric constant equivalent to that of pure water ice [Grima *et al.*, 2009].

[6] Up to six radar reflectors were traced and correlated between intersecting radargrams and gridded three-dimensional reflector surfaces were constructed (Figure 1a). Figure 2a shows an example of a typical (depth-corrected) SHARAD radargram with the six radar reflectors. We checked the data against clutter simulations and relocated subsurface reflections, taking into account the effects of surface slopes [Holt *et al.*, 2008]. The surface picked in the radargram was registered to the surface topography derived from Mars Orbiter Laser Altimeter (MOLA) data [Smith *et al.*, 2001] and then the reflector depth below the surface pick was calculated by converting two-way travel time to depth using the velocity of radar waves in pure water ice [Grima *et al.*, 2009].

[7] The following reflectors were traced: One reflector marking the transition from the multiple reflectors in the top  $\sim 400$  meters of the ice to a zone with no reflections. Two reflectors corresponding to the bottom of the second reflector package and three reflectors close to the bedrock. The observed reflectors are shown in Figures 2a and 3a.

[8] For the comparison with ice-flow modeling ice-flow, we assume that an internal reflector is an isochrone, i.e., marking a surface of the same age. The shape of an isochrone in a flowing ice cap is influenced by the mass balance (the deposition and/or removal of mass), basal conditions and the flow velocity of the ice. In order to clearly distinguish between observations and model results we refer to the observed stratigraphy as radar reflectors and the modeled

stratigraphy as isochrones. The age of isochrones in a flowing ice cap can be regarded as a transport equation and solved accordingly. Following, e.g., Hindmarsh *et al.* [2009], age is denoted  $X$  and the ageing equation is

$$\frac{\partial X}{\partial t} + \mathbf{v} \cdot \nabla X = 1, \quad (1)$$

where  $\mathbf{v}$  is the velocity field. The solution of this equation has been discussed in several studies [e.g., Greve *et al.*, 2002; Parrenin *et al.*, 2006]. In the model, ice flow is assumed to conform to the shallow ice flow approximation [e.g., Hutter, 1983] and the horizontal velocity can be set to be either constant with depth (plug flow) or varying due to the internal deformation of the ice. This is expressed by the velocity shape function  $v$ :

$$v(\zeta, \mathbf{r}) = 1, \quad \text{S} \quad (2)$$

$$v(\zeta, \mathbf{r}) = \frac{n+2}{n+1} \left( 1 - (1-\zeta)^{n+1} \right), \quad \text{ID} \quad (3)$$

where  $\mathbf{r} = (x, y)$ . The equations describe two situations; uniform plug flow (S) and isothermal internal deformation (ID) with flow exponent  $n = 3$  following Glen's flow law. The coordinate  $\zeta$  is the normalized elevation defined as  $\zeta(\mathbf{r}, z) = (z - b(\mathbf{r}))/H(\mathbf{r})$ , where  $z$  is the elevation,  $b(\mathbf{r})$  is the elevation of the bed, and  $H(\mathbf{r})$  is the total ice thickness.

[9] Plug flow often applies to areas with a high degree of basal melting where the ice essentially slides as one block over the bed topography. This bears resemblance to the scenario suggested by Fisher *et al.* [2010]. Internal deformation on the other hand, describes a scenario where there is negligible sliding and the horizontal velocity decreases with depth. Thus the horizontal velocity  $\mathbf{u}$  can be calculated from the expression  $\mathbf{u} = \bar{\mathbf{u}}v(\zeta, \mathbf{r})$  where  $\bar{\mathbf{u}}$  is the vertically averaged velocity. We investigate both scenarios with the assumption that the horizontal surface velocities are equal to the balance velocities calculated from the surface slope and the mass



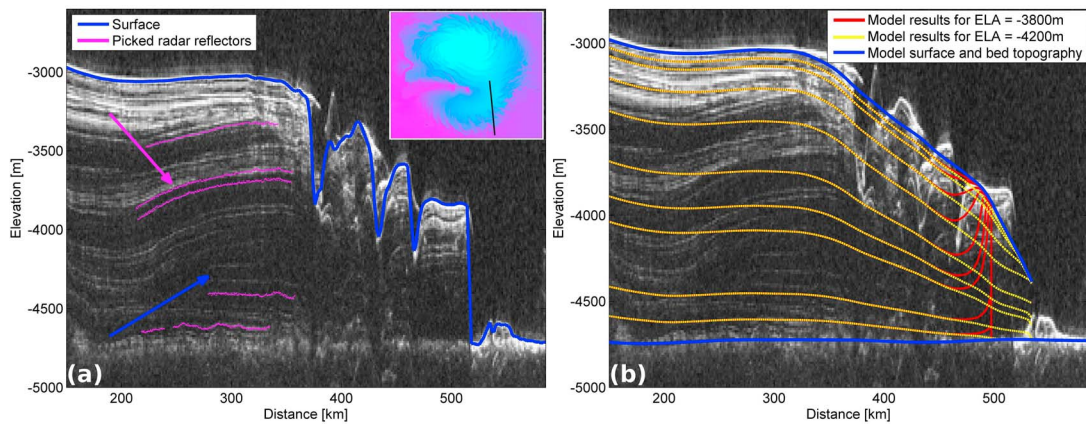


**Figure 2.** Depth-corrected radargram from line #52970100 with observed (a) radar reflections and (b) modeled isochrones. In Figure 2a the blue line is the MOLA-derived surface elevation along track (differences with radar first return are due to cross-track surface slope). The magenta arrow indicates the radar reflector whose full extent is mapped in Figure 1, the blue arrow shows the location of the unconformity discussed in the text.

balance (for information on calculating balance velocities see *Hindmarsh et al.* [2009]). The vertical velocity field is found using the continuity equation.

[10] As demonstrated by *Koutnik et al.* [2009] knowledge of surface and bed topography and internal stratigraphy is not sufficient to determine absolute accumulation rates. Thus we only concern ourselves with the accumulation pattern rather than the accumulation rate, further noting that the actual value of the accumulation only works as a scaling factor for the age of the isochrones, but does not impact their steady-state stratigraphy [*Parrenin et al.*, 2006; *Leysinger Vieli et al.*, 2011]. The isochrones are fitted to the radar reflectors using a least squares formulation. For more information on the model, fitting routine and the finite difference scheme solution see *Hindmarsh et al.* [2009].

[11] *Smith and Holt* [2010] concluded based on SHARAD stratigraphy that the central troughs and scarps of Planum Boreum do not post-date the deposition of the NPLD but are constructional features caused by aeolian processes concurrent with accumulation. However, in order to investigate

for ice flow and test the hypothesis of *Winebrenner et al.* [2008] we assume that the troughs and scarps of GL are a recent feature of the NPLD and that they have not co-existed with ice flow. Furthermore we assume that the overall shape of the NPLD as well as the mass balance are constant in time (i.e., a steady-state condition was achieved). Then we calculate the isochrones as they would appear under the influence of ice flow and mass balance. For surface topography, we use a smoothed version of the MOLA surface with a grid resolution of 28 km. The surface was reconstructed in such a way that it spans the topography across the troughs essentially filling in the depressions on the surface caused by the troughs. The bed topography was reconstructed from the bed picked in the radargrams and smoothed to the same resolution as the surface. Temperature is set to  $-100^{\circ}\text{C}$  which should represent current annual mean temperature reasonably well [e.g., *Paige et al.*, 1994; *Larsen and Dahl-Jensen*, 2000]. The temperature is unlikely to exert any significant influence on the stratigraphy of the isochrones. Gravity was set to  $3.69\text{ m/s}^2$  and the density of ice  $917\text{ kg/m}^3$ .

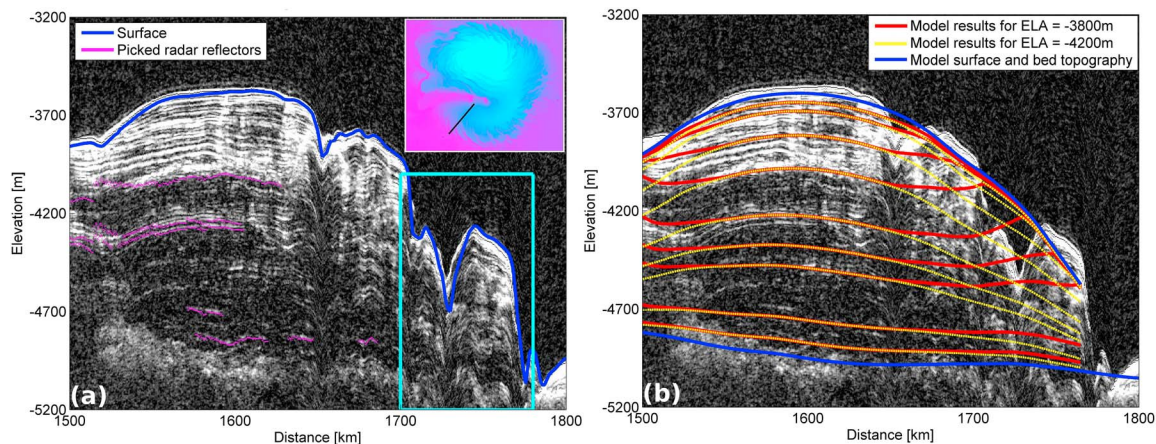


**Figure 3.** Depth-corrected radargram from line #51800200 with observed (a) radar reflections and (b) modeled isochrones. In Figure 3a the blue line is the MOLA-derived surface elevation along track (differences with radar first return are due to cross-track surface slope).

[12] Two scenarios are tested with the model, one where the accumulation is uniform over the entire ice cap and one where an area of ablation has been defined. *Milovich and Head* [2005] note that no evidence has been found for variation in accumulation rate with distance from the pole, while *Fishbaugh and Hvidberg* [2006] note a decreasing trend in accumulation with increasing distance from the pole. Here we adopt the approach by *Winebrenner et al.* [2008] and use uniform accumulation. Based on relict surface topography *Winebrenner et al.* [2008] reconstructed a potential mass balance distribution and identified areas of net ablation and net accumulation for 40 individual lines. The resulting mass balances were found to have equilibrium line altitudes (ELA, change in mass balance from mass gain to mass loss) of between  $-3800$  and  $-4200$  m. Based on this result we construct two scenarios with ablation, one for  $ELA = -3800$  m, i.e., where all points below  $-3800$  m are defined to be in an ablation zone and one for  $ELA = -4200$  m. The value of the ablation is set to half of the accumulation [*Winebrenner et al.*, 2008, Figure 4b] and the entire mass balance pattern is then smoothed by 2 grid points.

### 3. Observed Layer Stratigraphy

[13] Internal radar reflectors were clear and consistently visible in the majority of the SHARAD tracks (e.g., Figures 2a and 3a). Each reflector mapped was present, to some extent, in over 80% of the radargrams analyzed. Overall, the reflectors were smooth with no sudden dips toward bedrock or the ice surface. At the outer edges of GL the reflectors were often interrupted by surface clutter and gaps, both caused by steep trough topography; however, where radar tracks were more favorably oriented, internal stratigraphy was locally visible in the vicinity of troughs.

[14] Radar reflections in the upper NPLD exhibited significantly different morphology than in the lower part (Figures 2a and 3a). Lower radar reflections were more isolated as individual reflectors, rather than being grouped, and conformed to the nearly flat, more diffuse bed. We found no evidence of lower reflectors dipping toward the bed in this region, indicating that no zones of increased basal heating were present (at least not sufficient to melt ice from the bottom).

[15] Upper reflectors, grouped into radar-bright “packets”, generally conformed to the surface slopes, resulting in downwardly convex, parabola-like profiles. There was no evidence of upper reflectors intersecting or bending toward the surface, indicating that the reflectors are all in a former accumulation zone. If troughs represent ablation zones then one would expect the isochrones to bend upward toward the surface there [*Fisher*, 2000]; however, this is not the case. In other words, we find no evidence from the internal reflectors that the mass balance of GL has been dominated by “accumulation” (interchanging zones of accumulation and ablation) for substantial periods of time as suggested in other studies [e.g., *Fisher*, 2000].

### 4. Model Results and Discussion

[16] In the following, we compare the observed internal radar reflectors with results from the ice-flow model, focusing on two areas of GL: the so-called “saddle region” that connects the main lobe of the NPLD to GL, and westernmost GL (Figure 1a). Here we focus on the results from

the internal deformation scenario (equation (3)), however, the results from the scenario with basal sliding (equation (2)) do not differ significantly from this.

[17] As expected, the degree of fit for the lowermost reflectors was high. The lowermost reflectors experience the most vertical strain and are therefore likely to conform to the bed whether flow is present or not. Morphology of the uppermost reflectors would be altered by flow primarily in ablation zones, while the middle reflectors are likely to be the most sensitive overall indicators. In general, the fit between observed radar reflections and modeled isochrones is best in western GL and poorest in the saddle region (Figure 1b, see also Figure S1 in the auxiliary material); however, the misfit cannot be quantified in the areas where reflections could not be continuously tracked as discrete reflectors.<sup>1</sup> For this we rely on comparisons with radar profiles.

[18] In the saddle region, earlier studies have argued that the surface topography resembles that of an ice divide, as observed in Greenland and Antarctica [*Winebrenner et al.*, 2006], with ice potentially flowing from the main part of the NPLD into GL. However, *Holt et al.* [2010] found through mapping internal stratigraphy that rather than originating from southward mass transport, the initial construction of GL occurred early in NPLD history during an erosional episode that created an early version of Chasma Boreale. GL then grew as a separate depositional center, merging with the rest of the NPLD in the saddle region and farther to the northwest. The internal stratigraphy indicates that accumulation was continuous and largely uniform across this region, especially for the uppermost radar reflectors (Figure 2a), consistent with our assumption of overall uniform accumulation.

[19] Figure 2b shows the comparison of modeled isochrones with radar observations in the saddle region. The clear mismatch between the data and model for the middle and upper reflectors indicates that the hypothesized flow from the main NPLD lobe into GL is not correct given the assumptions of the model. The observed stratigraphies are, on the other hand, consistent with the middle and upper reflectors draping a dome-shaped unconformity surface in the lower reflectors, identified by *Holt et al.* [2010] and present in the saddle region (indicated with a blue arrow in Figure 2a). The presence of this elongate, dome-shaped feature in the subsurface might partly explain why the surface of GL seemingly resembles that of a recently flowing ice cap.

[20] In the westernmost part of GL we compared stratigraphy in 13 radargrams with that predicted by our model using the mass balance pattern suggested by *Winebrenner et al.* [2008] for the same region. The upper and lower elevation limits of their proposed ELA of  $-3800$  m and  $-4200$  m were investigated, and implemented as smooth transitions in the flow model. Note that the introduction of an ablation zone does not impact the isochrones upstream of the zone, only in the area of ablation close to the ice edge. Owing to the effects of trough topography on radar data acquisition (i.e., clutter and steep slopes), it was generally not possible to continuously map individual reflectors from the interior into the trough regions where the putative ablation zone is

<sup>1</sup>Auxiliary materials are available in the HTML. doi:10.1029/2011GL049630.



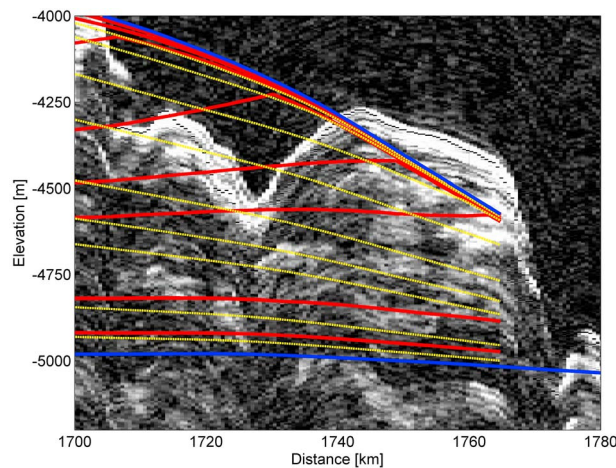


**Figure 4.** Expanded view of comparison at ice cap edge, as shown in Figure 3 (cyan box).

located; however, where SHARAD tracks were oriented most favorably the geometries of the radar reflections can be observed (e.g., Figure 3a) and compared with those modeled (Figure 3b). The comparison shows that the observed reflectors do not exhibit a change in slope as expected for isochrones situated in an ablation zone [cf. Koutnik *et al.*, 2009, Figure 6]. This is most evident for the case of ELA =  $-3800$  m, indicating that either ice flow has had very little influence on the stratigraphy of the reflectors or, if ice flow has influenced the stratigraphy there, ablation did not play a significant role.

[21] For ELA =  $-4200$  m, the overall match is better since both reflectors and isochrones are largely conformal to the surface. However, closer examination of the data (Figure 4) reveals that the radar reflectors clearly dip downward at a much steeper angle (compared to surface topography) than the isochrones. The apparent agreement between reflectors and isochrones is exaggerated by the difference between smoothed model surface and observed surface. The appearance of truncated reflectors is more likely due to recent erosional retreat from active mass-wasting events [Russell *et al.*, 2008]. If a past ablation zone existed below  $-4200$  m elevation when flow may have been active, it has been erased by more recent ablation.

[22] The surface-conformal stratigraphy in this area (Figure 4) also presents a problem for the flow hypothesis in the context of the troughs. Rather than the troughs truncating isochrones, as would be expected for the assumption of late-stage, post-flow trough formation [Winebrenner *et al.*, 2008], the observed reflectors drape trough topography (Figure 4). Therefore, the troughs must have existed prior to the deposition of the radar reflectors observed here. If flow did occur, then the troughs would need to have persisted during flow. Even if timescales for viscous relaxation could be accommodated [Pathare and Paige, 2005], observed reflectors do not match the upward-bending morphology expected beneath troughs coexisting with flow [Fisher, 2000].

[23] The introduction of a time-variable, non-uniform accumulation pattern could perhaps improve the agreement between radar reflectors and isochrones; however, there is no basis for invoking highly localized accumulation based on either current understanding of polar deposition [Fishbaugh *et al.*, 2008] or the observed lateral continuity of internal

reflectors. Overall, while the surface topography of the NPLD might have experienced some deformation in response to gravity, we find that the internal stratigraphy of Gemina Lingula is not consistent with an ice sheet that has previously experienced significant influence from ice flow (under the assumptions of our model). This implies that the NPLD has not been subjected to substantially warmer temperatures in the past and is mainly controlled by surface mass balance.

[24] **Acknowledgments.** This work was supported by NASA grant NNX08AR34G and the MRO Project through a SHARAD Co-I contract to JWH. NBK is supported by European Research Council grant 246815. The work was made possible with the support of the Antarctic Science Bursary, the Geological Remote Sensing Group, the Dudley Stamp Memorial Fund and the Department of Geography, University of Hull. The authors would like to thank D. Winebrenner for making the flowline data available to us and Ralf Greve and one anonymous reviewer, whose comments significantly improved this manuscript.

[25] The Editor wishes to thank Ralf Greve and an anonymous reviewer for their assistance in evaluating this paper.

## References

- Byrne, S. (2009), The polar deposits of Mars, *Annu. Rev. Earth Planet. Sci.*, **37**, 535–560.
- Clifford, S., et al. (2000), The state and future of Mars polar science and exploration, *Icarus*, **144**, 210–242, doi:10.1006/icar.1999.6290.
- Fishbaugh, K. E., and C. S. Hvidberg (2006), Martian north polar layered deposits stratigraphy: Implications for accumulation rates and flow, *J. Geophys. Res.*, **111**, E06012, doi:10.1029/2005JE002571.
- Fishbaugh, K. E., et al. (2008), Introduction to the 4th Mars Polar Science and Exploration Conference special issue: Five top questions in Mars polar science, *Icarus*, **196**, 305–317, doi:10.1016/j.icarus.2008.05.001.
- Fisher, D. A. (2000), Internal layers in an “accublation” ice cap: A test for flow, *Icarus*, **144**, 289–294.
- Fisher, D. A., M. H. Hecht, S. P. Kounaves, and D. C. Catling (2010), A perchlorate brine lubricated deformable bed facilitating flow of the north polar cap of Mars: Possible mechanism for water table recharging, *J. Geophys. Res.*, **115**, E00E12, doi:10.1029/2009JE003405.
- Greve, R., and R. Mahajan (2005), Influence of ice rheology and dust content on the dynamics of the north polar cap of Mars, *Icarus*, **174**, 475–485.
- Greve, R., Y. Wang, and B. Mugge (2002), Comparison of numerical schemes for the solution of the advective age equation in ice sheets, *Ann. Glaciol.*, **35**, 487–494.
- Greve, R., R. A. Mahajan, J. Segschneider, and B. Grieger (2004), Evolution of the north-polar cap of Mars: A modelling study, *Planet. Space Sci.*, **52**, 775–787, doi:10.1016/j.pss.2004.03.007.
- Grima, C., W. Kofman, J. Mouginot, R. J. Phillips, A. Hérique, D. Biccari, R. Seu, and M. Cutigni (2009), North polar deposits of Mars: Extreme purity of the water ice, *Geophys. Res. Lett.*, **36**, L03203, doi:10.1029/2008GL036326.
- Herkenhoff, K. E., and J. J. Plaut (2000), Surface ages and resurfacing rates of the polar layered deposits on Mars, *Icarus*, **144**, 243–253.
- Herkenhoff, K. E., S. Byrne, P. S. Russell, K. E. Fishbaugh, and A. S. McEwen (2007), Meter-scale morphology of the north polar region of Mars, *Science*, **317**, 1711–1715.
- Hindmarsh, R. C. A., G. J.-M. Leysinger Vieli, and F. Parrenin (2009), A large-scale numerical model for computing isochrone geometry, *Ann. Glaciol.*, **50**, 130–140.
- Holt, J. W., et al. (2008), Radar sounding evidence for buried glaciers in the southern mid-latitudes of Mars, *Science*, **322**, 1235–1238.
- Holt, J. W., et al. (2010), The construction of Chasma Boreale on Mars, *Nature*, **465**, 446–449, doi:10.1038/nature09050.
- Hutter, K. (1983), *Theoretical Glaciology: Material Science of Ice and the Mechanics of Glaciers and Ice Sheets*, D. Reidel, Dordrecht, Netherlands.
- Karlsson, N. B., D. M. Rippin, D. G. Vaughan, and H. F. J. Corr (2009), The internal layering of Pine Island Glacier, West Antarctica, from airborne radar-sounding data, *Ann. Glaciol.*, **50**, 141–146.
- Koutnik, M. R., E. D. Waddington, and D. P. Winebrenner (2009), A method to infer past surface mass balance and topography from internal layers in Martian polar layered deposits, *Icarus*, **204**, 458–470, doi:10.1016/j.icarus.2009.06.019.
- Larsen, J., and D. Dahl-Jensen (2000), Interior temperatures of the northern polar cap on Mars, *Icarus*, **144**, 456–462.
- Leysinger Vieli, G. J.-M. C., R. C. A. Hindmarsh, M. J. Siegert, and S. Bo (2011), Time-dependence of the spatial pattern of accumulation rate in East Antarctica deduced from isochronic radar layers using a 3-D

- numerical ice flow model, *J. Geophys. Res.*, **116**, F02018, doi:10.1029/2010JF001785.
- Milkovich, S. M., and J. W. Head III (2005), North polar cap of Mars: Polar layered deposit characterization and identification of a fundamental climate signal, *J. Geophys. Res.*, **110**, E01005, doi:10.1029/2004JE002349.
- Paige, D. A., J. E. Bachman, and K. D. Keegan (1994), Thermal and albedo mapping of the polar regions of Mars using Viking thermal mapper observations: 1. North polar region, *J. Geophys. Res.*, **99**, 25,959–25,991.
- Parén, J. G., and G. Robin (1975), Internal reflections in polar ice sheets, *J. Glaciol.*, **14**, 251–259.
- Parrenin, F., R. Hindmarsh, and F. Rémy (2006), Analytical solutions for the effect of topography, accumulation rate and lateral flow divergence on isochrone layer geometry, *J. Glaciol.*, **52**, 191–202.
- Pathare, A. V., and D. A. Paige (2005), The effects of Martian orbital variations upon the sublimation and relaxation of north polar troughs and scarps, *Icarus*, **174**, 419–443.
- Phillips, R. J., et al. (2008), Mars north polar deposits: Stratigraphy, age, and geodynamical response, *Science*, **320**, 1182, doi:10.1126/science.1157546.
- Putzig, N. E., et al. (2009), Subsurface structure of Planum Boreum from Mars Reconnaissance Orbiter Shallow Radar soundings, *Icarus*, **204**, 443–457, doi:10.1016/j.icarus.2009.07.034.
- Rippin, D. M., M. J. Siegert, J. L. Bamber, D. G. Vaughan, and H. F. J. Corr (2006), Switch-off of a major enhanced ice flow unit in East Antarctica, *Geophys. Res. Lett.*, **33**, L15501, doi:10.1029/2006GL026648.
- Russell, P., et al. (2008), Seasonally active frost-dust avalanches on a north polar scarp of Mars captured by HiRISE, *Geophys. Res. Lett.*, **35**, L23204, doi:10.1029/2008GL035790.
- Seu, R., et al. (2007), SHARAD sounding radar on the Mars Reconnaissance Orbiter, *J. Geophys. Res.*, **112**, E05S05, doi:10.1029/2006JE002745.
- Siegert, M. J., A. J. Payne, and I. Joughin (2003), Spatiotemporal stability of Ice Stream D and its tributaries, West Antarctica, revealed by radio-echo sounding and interferometry, *Ann. Glaciol.*, **37**, 377–382.
- Smith, D. E., et al. (2001), Mars Orbiter Laser Altimeter: Experiment summary after the first year of global mapping of Mars, *J. Geophys. Res.*, **106**, 23,689–23,722.
- Smith, I. B., and J. W. Holt (2010), Onset and migration of spiral troughs on Mars revealed by orbital radar, *Nature*, **465**, 450–453.
- Tanaka, K. L., J. A. P. Rodriguez, J. A. Skinner Jr., M. C. Bourke, C. M. Fortezzo, K. E. Herkenhoff, E. J. Kolb, and C. H. Okubo (2008), North polar region of Mars: Advances in stratigraphy, structure, and erosional modification, *Icarus*, **196**, 318–358.
- Winebrenner, D., M. Koutnik, E. Waddington, A. Pathare, B. Murray, S. Byrne, and J. Bamber (2006), Evidence for past flow in the Martian north polar layered deposits from ice flow inverse modeling, *Lunar Planet. Sci. Conf.*, **37th**, Abstract 1875.
- Winebrenner, D. P., M. R. Koutnik, E. D. Waddington, A. V. Pathare, B. C. Murray, S. Byrne, and J. L. Bamber (2008), Evidence for ice flow prior to trough formation in the Martian north polar layered deposits, *Icarus*, **195**, 90–105.
- R. C. A. Hindmarsh, British Antarctic Survey, High Cross, Madingley Road, Cambridge CB3 0ET, UK.
- J. W. Holt, Institute for Geophysics, Jackson School of Geosciences, University of Texas at Austin, 1 University Stn. C1160, Austin, TX 78712-0254, USA.
- N. B. Karlsson, Centre for Ice and Climate, Niels Bohr Institute, University of Copenhagen, Juliane Mariesvej 30, DK-2100 Copenhagen, Denmark. (nanna.karlsson@nbi.ku.dk)